

Design, Development, and Validation of an Intake System for an FSAE Racecar



Saliq Shamim Shah, Kshitij Singh, Leenus Jesu Martin,
and M. Jerome Stanley

Abstract The aim of this paper is to design the intake system for an engine to optimize the performance of restricted KTM 390-supported powertrains of a Formula Society of Automotive Engineers (FSAE) combustion car of team Camber Racing. Keeping in a view the safety of students, power produced by the engine is restricted by inclusion of a 20 mm air restrictor. It is made mandatory for all the student teams to participate in the racing event. With a goal of exploring and understanding various parameters involved in modeling a 20 mm air restrictor which is to be incorporated in the intake of 390 cc KTM single-cylinder engine, the required engine performance need to be attained. Analysis is done with the help of the CFD software ANSYS Fluent. With the incorporation of air restrictor upstream the intake system, pressure loss is observed. This in turn reduces the volumetric efficiency of the engine significantly. The goal of the intake system was to reduce the pressure loss caused due to restriction and to provide a reservoir to act as an infinitely large reservoir of air, to improve the breathing characteristics of engine (Hadjkacem et al., Arab J Sci Eng 2018). The constraint was engine response delay. The volumetric efficiency could have been further improved but would have been detrimental to engine response time (Mattarelli and Rinaldini in SAE Technical Paper 01-0833:2012, 2012 [1]).

Keywords FSAE · Intake · Plenum · IC engine · KTM 390

S. S. Shah · K. Singh

Department of Mechanical Engineering, College of Engineering and Technology, SRM Institute of Science and Technology, Tamil Nadu, Kattankulathur, Kanchipuram 603203, India

L. J. Martin · M. Jerome Stanley (✉)

College of Engineering and Technology, SRM Institute of Science and Technology, SRM Nagar, Kattankulathur, Kanchipuram, Chennai, Tamil Nadu 603203, India

e-mail: stanleystallion07@gmail.com

1 Introduction

Volumetric efficiency is a parameter that defines the performance of an internal combustion engine [2]. Going by the rule of thumb, higher the volumetric efficiency higher the power. That being the reason of the rule incorporated by the Formula Society of Automotive Engineers hereafter referred as FSAE. Keeping in view the safety of students and to challenge the engineering caliber of students, the air restrictor of 20 mm was made a necessity for an FSAE car to restrict the power that IC engine can produce. According to the rules, the intake setup for a naturally aspirated FSAE car should be as shown in Fig. 1 and that in turbocharged car is shown in Fig. 2.

Taking in the consideration of the team goals of FSAE combustion team Camber Racing of building a “Light Weight Agile Car,” the design decision of using a naturally aspirated system was done. According to the rules, the design had to be throttle body followed by a restrictor, a plenum, a runner, and finally the engine. Accordingly, the design was started.

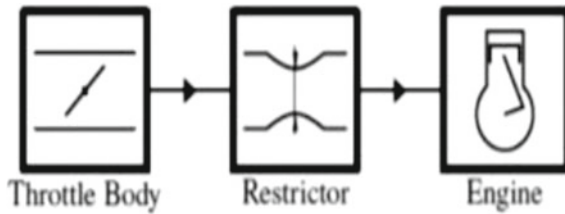


Fig. 1 FSAE rules for naturally aspirated engine

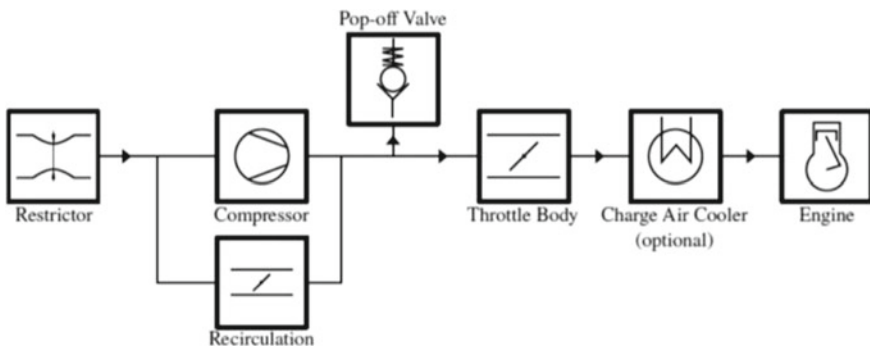


Fig. 2 FSAE rules for turbocharged engine

2 Restrictor

While designing a restrictor, there were two ways to do it. First one being the Orifice plate and other being the Converging Diverging Nozzle [3]. The aim of the design was to maximize the pressure recovery between the restriction and the restrictor outlet. There was a significant drop in pressure of air since it flows through the restriction. The goal was to gradually bring the air back to as high a pressure as possible near the engine inlet so as to maximize volumetric efficiency of the engine.

Orifice Plate

This is a plate with a circular hole in the middle. In this scenario, “*vena contracta*” is observed. This is the decrease in cross section area of the flow at the orifice. This effect brings two issues. Firstly, since the cross section for flow is decreased the flow gets choked much more “quickly” than otherwise. Secondly since the flow through the restriction effectively increases, the pressure becomes lower than before. As a result, greater pressure recovery would be needed. It had a coefficient of discharge of 0.6.

Converging Diverging Nozzle

In the case of a convergent divergent nozzle, the flow is gradually accelerated as it is sent to the restriction and then the flow gradually regains the pressure as it exits out through the diverging section. The downside of CD nozzle was that it induced higher amounts of drag when compared to the orifice plate. This is because it has more surface area in contact with the flow. It had coefficient of discharge of 0.99 which is way higher than orifice plate.

Comparison of orifice plate to the CD nozzle was done; it was evident that the CD nozzle recovers pressure more effectively than the orifice plate. The CD nozzle has a higher coefficient of discharge than the orifice plate. Hence, we decided to make our restrictor in the form of a Convergent Divergent nozzle. After the decision was done, ANSYS fluent model was created to understand and quantify the pressure losses. Diverging angles of 6°, 9°, 12°, and 15° were studied (Figs. 3 and 4), and the results were tabulated in Table 1.

Hence, a diverging angle of 6° was selected for the restrictor. When the downstream pressure in the orifice is decreased and the mass flow rate of fluid keeps increasing until it reaches the velocity of air reaches $mac = 1$ at the throat. On further decreasing the pressure downstream, the mass flow rate stagnates and that point is said to be choke point. Using the compressible flow equation shown below, we can calculate the mass flow rate at choking point for a 20 mm restriction

$$\dot{m} = \frac{AP_t}{\sqrt{T_t}} \times \sqrt{\frac{\gamma}{R}} M \left(1 + \frac{\gamma - 1}{2} M^2 \right)^{-\frac{\gamma+1}{2(\gamma-1)}}$$

Here, the values were taken as follows:

$$P_t = 101325 \text{ Pa} \quad T_t = 300 \text{ K} \quad \gamma = 1.4$$

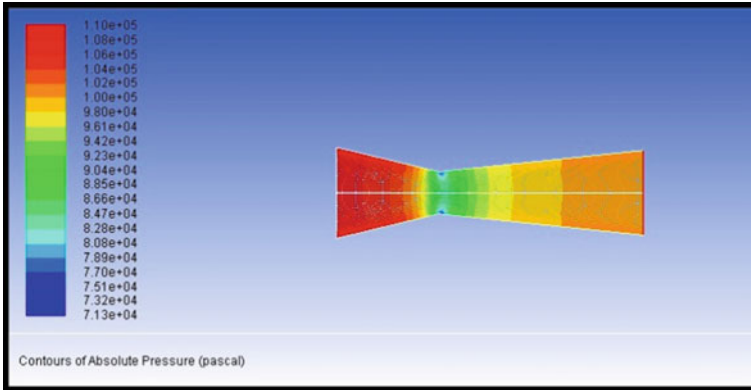


Fig. 3 Pressure contour for 6°

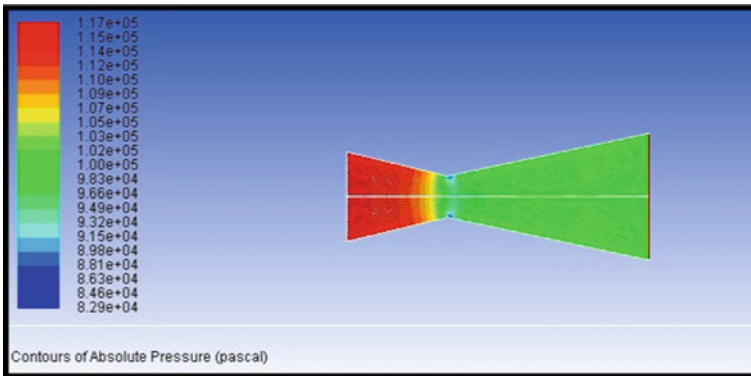


Fig. 4 Pressure contour for 12°

Table 1 Diverging angles

S. No.	Diverging angles (°)	Pressure loss (Pa)
1	6	298.845
2	9	381.921
3	12	487.63
4	15	568.378

$$R \text{ (air)} = 0.287 \text{ kJ/Kg-K}$$

$$A = \pi r^2 = 0.000314 \text{ m}^2 \text{ [Here } r = 20 \text{ mm].}$$

$$M = 1$$

From the calculations, the mass flow rate was found to be 0.074 kg/s.

For KTM 390 engine, RPM at the Choke Point

$$\text{RPM} = x$$

$$\text{CPM} = x/2$$

$$\text{CPS} = \text{Intake Strokes/s} = (x/2)/60 = x/120$$

$$\rho = \text{Density} = 1.2 \text{ kg/m}^3$$

$$\dot{m} = 0.074 \text{ kg/s}$$

$$\text{Volume of air/sec} = (x/120)(373.2/1000) \text{ L}$$

$$(0.074/0.00012) = (x/120)(373.2/1000)$$

$$x = 19,870 \text{ RPM}$$

RPM: Rotation per minute

CPM: Cycle per minute

CPS: Cycle per second

From the calculations, the choke point RPM was found to be 19,870 RPM.

3 Plenum

To decrease the impact of the restrictor on airflow, it is important to limit the most fast moving air particles. An approach to achieve this goal is to put a plenum between the restrictor and the prime mover. The plenum permits to limit the pulsating flow through the restrictor. As a result, the pressure loss at the restrictor diminishes and the mass flow rate to the prime mover ascends, thus increasing the volumetric efficiency of the IC engine. Higher the volume of plenum, higher the power produced by the engine. Then again, with increase in volume of plenum the engine response time increases and thus the concept of throttle lag. If put in those exact words, power requested by the driver is supplied after a time lag, thus detrimental to the driveability. A similar issue happens during decelerations when the brake torque helps reduce vehicle speed. The restrictor on the intake system affects single-cylinder engines more than multi-cylinder engines, due to their great pulsating mass flow. To determine the plenum volume, an iterative experimental setup is manufactured and implemented on team Camber Racing's FSAE racecar. A PVC model of intake is manufactured, and the volume is reduced in increments. A data logger AIM EVO 4 of the team is used to monitor manifold absolute pressure (MAP) (Fig. 6), throttle position (TP). The MAP sensor is placed on the runner as near to the flange of engine as possible considering packaging constraints. A compromise is done between MAP and the engine response time by monitoring throttle position and RPM (Fig. 7), thus fulfilling the initial goals of the plenum (Fig. 5).

The plenum was decided to be 2.8 L. The shape of the plenum aids in having a better flow in the intake system improving the volumetric efficiency. Two designs of plenum were investigated, one was a rectangular-shaped plenum while the other was Bezier curve-based plenum. The volume and length of the two designs were kept same, and CFD analysis was done along with the restrictor portion. A bell mouth was used at the inlet end of runner in the plenum. This was done in order to decrease vena contracta effect [4, 5]. From the analysis, the outlet velocity of the Bezier curve plenum was greater than the rectangular one [6] (Figs. 8, 9, 10, and 11).



Fig. 5 PVC Intake iterative setup

		Enable Fuel		Setup Tracer		Clear Tracer		RPM																	
		0	600	1000	1500	2000	2500	3000	3600	4000	4500	5000	5500	6000	6500	7000	7500	8000	8500	9000	9500	10000	10500		
MAP (PSI)	105.0	1.69	1.78	1.88	1.97	2.25	2.53	2.81	3.19	3.38	3.56	3.56	3.56	3.66	3.66	3.66	3.75	3.84	3.84	3.94	3.94	3.84	3.84		
	101.2	1.69	1.78	1.88	1.97	2.25	2.44	2.72	3.09	3.28	3.47	3.47	3.47	3.56	3.56	3.56	3.66	3.75	3.75	3.84	3.84	3.75	3.75		
	97.4	1.59	1.69	1.78	1.88	2.16	2.44	2.72	3.09	3.19	3.38	3.38	3.38	3.47	3.47	3.47	3.56	3.66	3.66	3.75	3.75	3.66	3.66		
	93.6	1.59	1.69	1.78	1.88	2.16	2.34	2.63	3.00	3.19	3.28	3.28	3.28	3.38	3.38	3.38	3.47	3.47	3.47	3.56	3.56	3.47	3.47		
	89.8	1.59	1.69	1.78	1.88	2.06	2.34	2.53	2.91	3.09	3.28	3.19	3.19	3.28	3.28	3.28	3.28	3.38	3.38	3.47	3.47	3.38	3.38		
	86.0	1.50	1.59	1.69	1.78	2.06	2.25	2.53	2.81	3.00	3.19	3.19	3.09	3.19	3.19	3.19	3.19	3.19	3.28	3.28	3.38	3.38	3.28	3.28	
	82.2	1.50	1.59	1.69	1.78	1.97	2.25	2.44	2.81	2.91	3.09	3.09	3.00	3.09	3.09	3.00	3.09	3.19	3.19	3.19	3.28	3.28	3.19	3.19	
	78.4	1.50	1.59	1.69	1.78	1.97	2.16	2.34	2.72	2.81	3.00	3.00	3.00	3.00	3.00	3.00	2.91	3.00	3.09	3.09	3.09	3.00	3.00	3.00	
	74.6	1.41	1.50	1.59	1.69	1.97	2.16	2.25	2.63	2.81	2.91	2.91	2.91	2.91	2.91	2.91	2.81	2.91	2.91	2.91	3.00	3.00	2.91	2.91	
	70.8	1.41	1.50	1.59	1.69	1.88	2.06	2.25	2.63	2.72	2.81	2.81	2.81	2.81	2.81	2.72	2.81	2.81	2.81	2.91	2.91	2.81	2.81	2.81	
	67.0	1.41	1.50	1.78	1.88	2.06	2.06	2.16	2.53	2.63	2.81	2.72	2.72	2.72	2.72	2.63	2.72	2.72	2.72	2.81	2.81	2.72	2.72	2.72	
	63.2	1.31	1.41	1.78	1.78	1.97	2.06	2.06	2.44	2.53	2.72	2.63	2.63	2.63	2.63	2.53	2.53	2.63	2.63	2.63	2.63	2.63	2.53	2.53	
	59.4	1.31	1.41	1.69	1.78	1.97	1.97	2.06	2.34	2.44	2.63	2.53	2.53	2.53	2.53	2.44	2.44	2.53	2.53	2.53	2.53	2.44	2.44	2.44	
	55.6	1.31	1.41	1.69	1.78	1.88	1.97	1.97	2.34	2.44	2.53	2.53	2.44	2.44	2.34	2.34	2.34	2.44	2.44	2.44	2.44	2.44	2.34	2.34	
	51.8	1.31	1.31	1.69	1.78	1.88	1.88	1.97	2.25	2.34	2.44	2.44	2.34	2.34	2.25	2.25	2.25	2.25	2.25	2.25	2.34	2.34	2.25	2.25	
	48.0	1.22	1.31	1.59	1.69	1.78	1.88	1.88	2.16	2.25	2.34	2.34	2.25	2.25	2.16	2.16	2.16	2.16	2.16	2.16	2.16	2.16	2.06	2.06	
44.2	1.22	1.31	1.41	1.50	1.59	1.78	1.78	2.06	2.16	2.34	2.25	2.16	2.16	2.06	2.06	2.06	2.06	2.06	2.06	2.06	2.06	1.97	1.97		
40.4	1.22	1.31	1.41	1.50	1.59	1.78	1.78	2.06	2.06	2.25	2.16	2.06	2.06	1.97	1.97	1.97	1.97	1.97	1.97	1.97	1.88	1.88	1.88		
36.6	1.13	1.22	1.31	1.41	1.50	1.69	1.69	1.97	2.06	2.16	2.06	1.97	1.97	1.88	1.88	1.78	1.88	1.88	1.88	1.88	1.78	1.78	1.78		
32.8	1.13	1.22	1.31	1.41	1.50	1.69	1.69	1.88	1.97	2.06	1.97	1.97	1.88	1.78	1.69	1.69	1.69	1.69	1.69	1.69	1.78	1.78	1.59	1.59	
29.0	1.13	1.22	1.31	1.41	1.41	1.59	1.59	1.88	1.88	1.97	1.88	1.88	1.78	1.69	1.59	1.59	1.59	1.59	1.59	1.59	1.59	1.50	1.50		

Fig. 6 RPM VS Manifold absolute pressure table

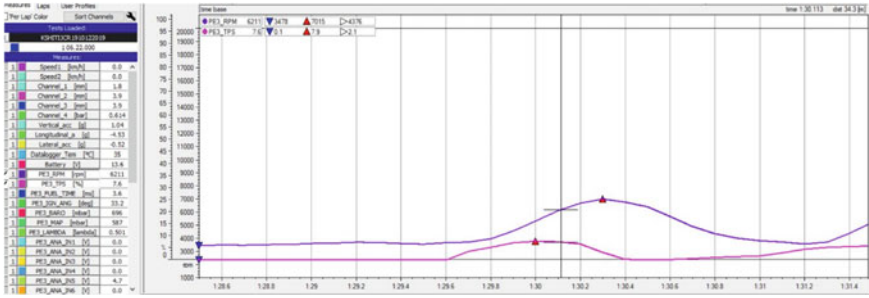


Fig. 7 Throttle position versus RPM plot

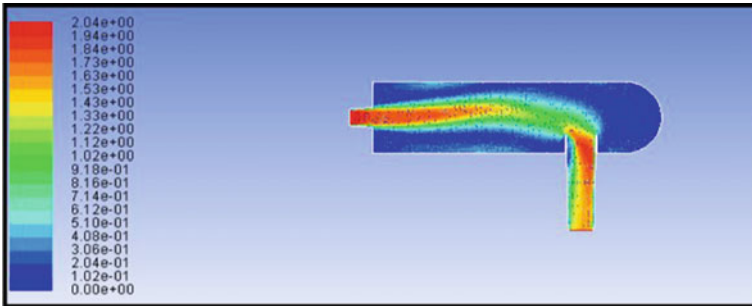


Fig. 8 Velocity contour for rectangular plenum without bell mouth

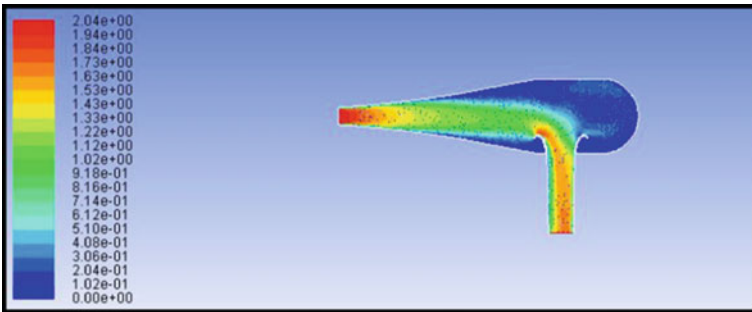


Fig. 9 Velocity contour Bezier curved plenum with bell mouth

Structural Design

An accelerometer was placed on the end of the plenum, and the car was run. Maximum acceleration was found to be 3G's. A structural simulation was run to study stress, strain, and FOS on the plenum (Figs. 12 and 13).

Various materials and manufacturing techniques were taken into consideration (Table 2). The manufacturing of the plenum was done through SLS process using

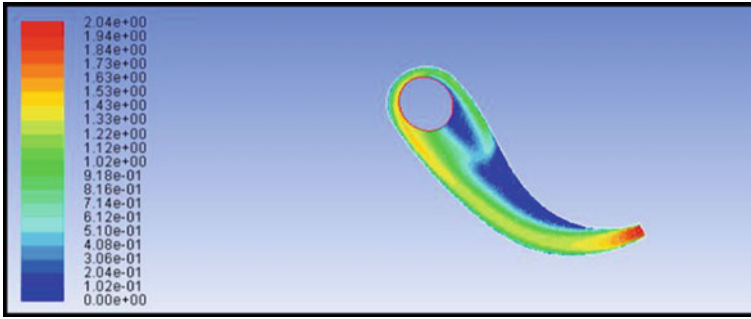


Fig. 10 Velocity contour Bezier curved plenum with bell mouth and a bend

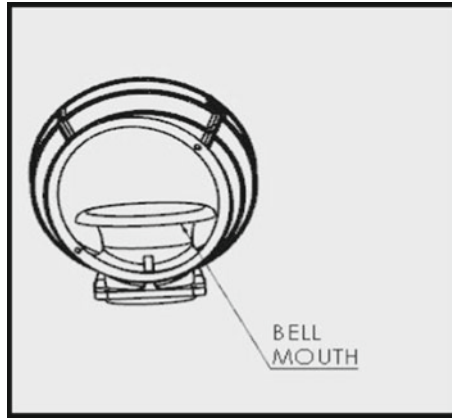


Fig. 11 Bell Mouth

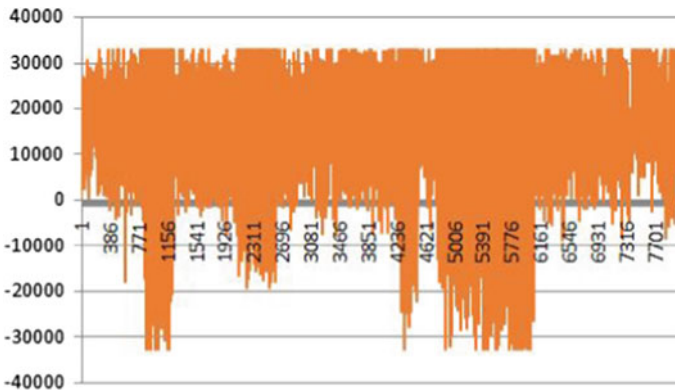


Fig. 12 Accelerometer plot

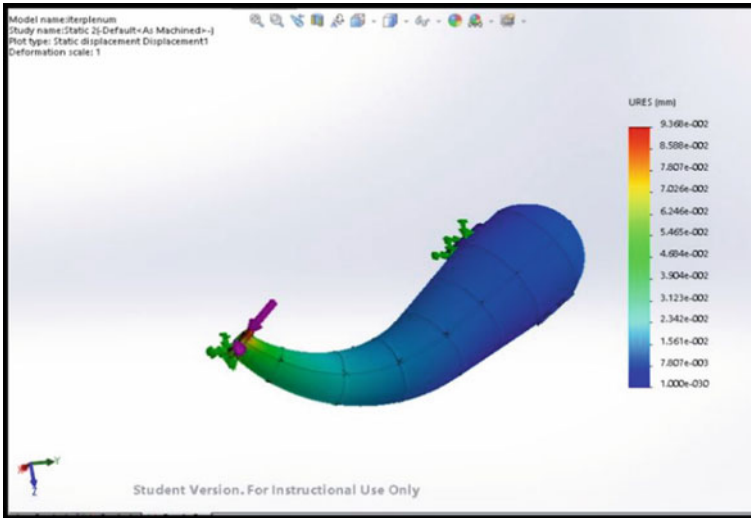


Fig. 13 Finite element analysis of the plenum

Table 2 Material decision matrix

Process	Nylon 12 (SLS)	PC (FDM)	PC-ABS (FDM)	ULTEM 9085 (FDM)
Tensile strength (MPa)	48	68	41	72
Flexural strength (MPa)	47	104	68	115
Heat deflection temperature	95	138	96	153
Tensile modulus (MPa)	1650	2280	Na	na
Flexural modulus (MPa)	1500	2234	1931	2507
Fatigue resistance	High number of cycles	very low	Average	Average
Cost and availability	Average/common	Average/common	Average/abundant	High/rare

Nylon12 material. This was chosen over other methods like FDM because of the superior finish and quality of the product. Conventional techniques were not used due to the complex geometry and its high weight.

4 Runner

Runner is essentially a connection between plenum and engine. The Helmholtz frequency is the frequency at which the “Ram effect” happens in the intake runner, subsequently giving a more prominent mass of air into the chamber; thus, the volumetric efficiency and subsequently other performance parameters like power torque curve get enhanced. The relationship is such that the frequency of Helmholtz is double the RPM of the engine; the Ram impact builds the volumetric efficiency. The thought was to decide the Helmholtz frequency for a particular runner length for a particular RPM band for which this length offers the highest volumetric efficiency. For drivetrain targets of the team Camber Racing, the operating RPM band was selected to be 8000 RPM. The valve-timing diagram of the KTM 390 engine was studied. The time for closing of intake valve at 8000 RPM is studied. Speed of acoustic was found using a data book at ambient temperatures. Thus, the wavelength of wave is found. It was found to be 1.88 m. This was fundamentally impossible to package in the template of car. Considering the packaging, 8th harmonic of the said wave was used. It was calculated to be 0.235 m, and this could be effectively packaged. Hence, 0.235 m of runner length was selected. The stock runner was reverse engineered, and the injector angle was found. It was found to be 36.5° with respect to the runner axis. A MAP sensor was placed as close to the engine flange as possible so as to get the precise pressure data (Fig. 14).

The runner was a crucial part of the intake in which spontaneous fires could occur; hence, a fire- and fuel-resistant material ULTEM 9085 was considered but due to the high cost and lack of availability an aluminum runner was made. The aluminum portion of runner length was 107 mm because of the port on the engine had a length of 79 mm and bell mouth of 41 mm length was integrated with the plenum.

Fig. 14 KTM 390 Valve timing diagram

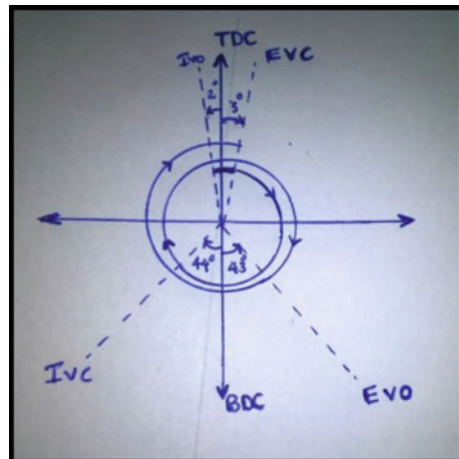


Table 3 Comparison

Parameter	KTM 390 stock	Camber racing's racecar
Peak power	42.9 BHP @ 9000 rpm	47.5 BHP@ 9500RPM
Peak torque	37 Nm@ 7000RPM	34.1 Nm @ 9500RPM

**Fig. 15** Commercial eddy current dynamometer

5 Validation

To validate the intake system and powertrain as a whole, Camber Racing's racecar was taken to a chassis eddy current dynamometer, and multiple runs were done on part load and full load conditions. The comparative data of stock KTM 390 and Camber Racing's powertrain design has been tabulated in Table 3. On observing the power and torque data of stock KTM 390 and customized KTM 390 powertrain, it was observed that even after running restricted intake setup as mandated by the FSAE rules, higher power figures were achieved. That was possible only if higher volumetric efficiency is achieved and hence the intake system was validated [5] (Figs. 15 and 16).

6 Conclusion

Formula society of automotive engineers imposes a rule of incorporation of 20 mm restrictor into the intake system downstream the throttle valve, which is detrimental not only to pressure downstream the restrictor but also the volumetric efficiency of the engine. This poses an engineering challenge to recover the pressure effectively while maintaining the engine response. This paper undertakes the challenge to

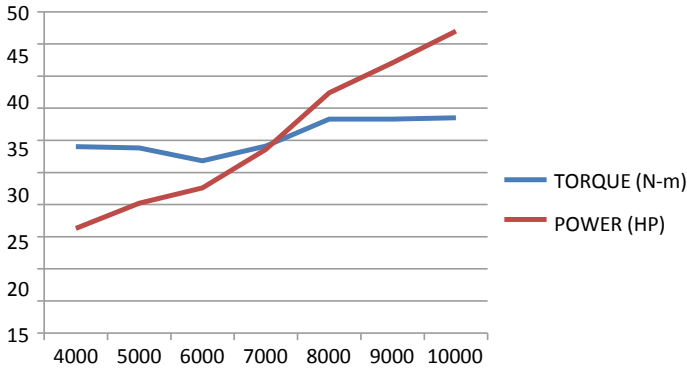


Fig. 16 Power torque graph of camber racing customized powertrain

design, develop, and validate an intake system to model the restrictor in a way that could maximize the pressure recovery after the restrictor and improve the volumetric efficiency of the engine while maintaining the engine response. In this paper, work was to make a best possible compromise between the maximum power and engine response time. On analyzing the data, it was found that the engine response time was found to be 0.02 s (Figs. 17 and 18).

Fig. 17 CAD model of Intake system

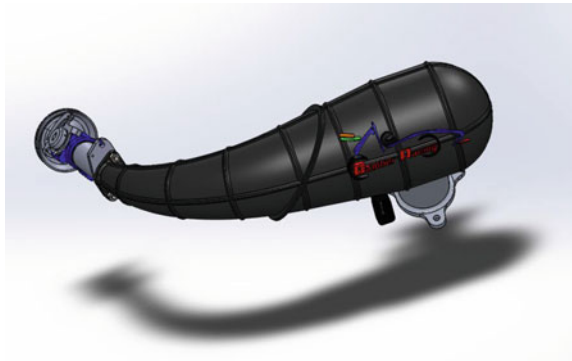


Fig. 18 Real Intake system



Acknowledgements The authors would like to thank the official combustion team of SRM Institute of Science and Technology, Camber Racing for their unconditional support. The authors would also like to thank the Automobile Department for giving us the unconditional support.

References

1. Hadjkacem S, Ali M, Mohamed J, Abid S (2018) Volumetric efficiency optimization of manifold with variable geometry using acoustic vibration for intake manifold with variable geometry in case of LPG-enriched hydrogen engine. Arab J Sci Eng
2. Biancolini M (2007) Engine/vehicle matching for a FSAE race car. SAE Technical Paper 2007: 01-3541
3. Mattarelli E, Rinaldini C (2012) Development of a high performance engine for a formula SAE Racer. SAE Technical Paper 2012: 01-0833
4. Hamilton L, Lee J (2009) The effects of intake plenum volume on the performance of a small normally aspirated restricted engine. SAE Int J Engines 1:1312–1318
5. Cauchi J, Farrugia M, Balzan N (2006) Engine simulation of a restricted FSAE engine, focusing on restrictor modelling. SAE Technical Paper 2006: 01-3651
6. Yan F, Wang J (2012) Pressure-based transient intake manifold temperature reconstruction in diesel engines. Control Eng Pract 20:531–538